Swantje Pietsch[1,*]
Michael Schönherr[2]
Frank Kleine Jäger[2]
Stefan Heinrich[1]

Measurement of Residence Time Distributions in a Continuously Operated Spouted Bed

Continuous gas-solid processes are applied in many industries with particulate products, e.g. for granulation or coating. In this contribution, the residence time behavior in a continuously operated prismatic spouted bed was determined by applying an impulse of magnetizable tracer particles. Experiments were performed with the original configuration and with separation plates including mouse holes of varying size between the different chambers of the ProCell 25 apparatus. It is shown that the shape of the residence time distribution is influenced by the separation plates. In order to quantify the backmixing between the chambers, discontinuous experiments were performed, and the bed mass distribution and the distribution of the tracer were measured and compared to the initial conditions.

Keywords: Backmixing, Chamber separation, Horizontal spouted bed, Magnetizable tracer particles, Residence time distribution

Received: August 16, 2019; *revised:* February 24, 2020; *accepted:* March 2, 2020

DOI: 10.1002/ceat.201900453

1 Introduction

1.1 Spouted-Bed Process

One of the most common gas-solid processes is the fluidized-bed technology, whose origin lies in 1922, when it was developed as gasifier by Fritz Winkler [1]. Nowadays, fluidized beds are widely applied in several industrial fields, e.g. in chemical engineering, combustion, or in the pharmaceutical and food industry. The solid is entrained by an upwards gas flow through a distributor plate and fluidized, which makes it look like a boiling liquid. Especially very small or very big particles, or those with non-spherical shape or high cohesiveness, are often difficult to fluidize in a classical fluidized bed. For these particles, the spouted bed, introduced by Mathur and Gishler in 1954 [2], has been established. In contrast to a fluidized bed, the gas enters the process chamber via slits or tubes instead of a distributor plate over the whole cross-sectional area, resulting in much higher gas and particle velocities in the area of the gas inlet. The particles move upwards in this spout zone. With increasing height, the cross-section of the chamber increases, which results in a deceleration of the velocity and finally a downwards movement of the particles along the apparatus walls. Afterwards, the particles are accelerated from the dense annulus zone back into the spout zone, which causes the fountain-like flow behavior. This flow pattern and the involved high velocities come along with an improved heat, mass, and momentum transfer [3]. Since its invention, different types of spouted beds have been developed, which are categorized as axisymmetric, asymmetric, or slot-rectangular. The three-dimensional apparatus investigated in this work can be assigned to the category of slot-rectangular spouted beds and is often termed as prismatic. The prismatic shape has the advantage that the scale-up possibility is enhanced by increasing the depth of the apparatus.

Gas-solid processes including spouted beds can be performed in batch or continuous operation, whereby throughputs between $20\,kg\,h^{-1}$ and $10\,t\,h^{-1}$ are common [4]. Due to their higher throughput and productivity, continuously operated processes are often preferred in the chemical industry. Large apparatuses for continuous operation frequently consist of several chambers that are serially connected. With this configuration, different unit operations, such as granulation, coating, and drying, can be realized consecutively in one device. The ProCell 25 apparatus from the manufacturer Glatt GmbH (Germany) consists of four different chambers, which are characterized by having a separate gas inlet and a nozzle each. This configuration allows, e.g., the granulation in the first chamber, the application of two different coating agents in the second and third chambers, and the final drying step in the fourth chamber, with individual superficial gas velocities at the inlet of each section. The serial connection of unit operations in one

[1]Dr.-Ing. Swantje Pietsch, Prof. Dr.-Ing. habil. Dr. h.c. Stefan Heinrich
swantje.pietsch@tuhh.de
Institute of Solids Process Engineering and Particle Technology, Hamburg University of Technology, Denickestrasse 15, 21073 Hamburg, Germany.

[2]Dr.-Ing. Michael Schönherr, Prof. Dr.-Ing. Frank Kleine Jäger
BASF SE, RCP/MK – L540, Carl-Bosch-Strasse 38, 67056 Ludwigshafen am Rhein, Germany.

plant requires a certain residence time of the particles not only in the whole apparatus but also in the different stages, to ensure a constant and homogeneous product quality. This means, for example, that the coating layer is of the required thickness or that the drying is conducted until a certain residual moisture content is obtained. In addition, backmixing has to be avoided as already coated particles should not return into the granulation zone but should enter the drying area, or dried particles should not go back to the coating step. In order to measure and adjust the movement of particles through continuous processes, the knowledge of residence time distributions (RTD) is of great importance.

1.2 Residence Time Distributions

The residence time is defined as the time that a particle needs to get from the inlet of the apparatus to its outlet. For the description of residence time behavior, ideal and real reactors are distinguished [5]. In case of ideal reactors, two defined borderline cases do exist: the ideal stirred-tank reactor and the ideal plug-flow reactor. In ideal stirred-tank reactors, a perfect micro-mixing is assumed, resulting in a homogeneous concentration independent of the place in the plant at every time. In continuously operated ideal stirred-tank reactors, each and every particle spends the same time in the apparatus. Ideal plug-flow reactors, on the other hand, are based on the flow of a flat profile, which results in concentrations that are time dependent but independent of the location in the plant. Again, every particle needs the same time for passing the reactor. The behavior of particles in real reactors deviates from perfect micro-mixing and from perfect velocity profiles, which is caused by the different flow velocities of fluids, dead zones, and bypasses. As a consequence, the RTD represents the range of time that particles will need from the inlet to the outlet. For quantification of the residence time behavior, exit age distributions are used, whereby the number of particles leaving the reactor in the time interval Δt is plotted against the time t.[1)] It is assumed that the flow is stationary and incompressible (ρ_f = const.), the transports at the inlet and outlet are caused by forced convection, and that the boundary condition "closed-closed" is valid [6]. This condition means that a particle that has entered the plant is not able to leave it through the inlet again and that a particle that has left the reactor through the outlet cannot enter it again. The dimensionless value $F(t)$ gives the fraction of particles that spends a given duration t in the plant, whereby after an infinitely long period all particles have left the reactor:

$$F(t) = \int_0^t E(t)\mathrm{d}t \tag{1}$$

$$\int_0^\infty E(t)\mathrm{d}t = 1 \tag{2}$$

The first moment μ_1 of the exit age distribution gives the mean residence time $\bar{t}$ of the particles in the apparatus:

$$\mu_1 = \bar{t} = \int_0^\infty t^1 E(t)\mathrm{d}t \tag{3}$$

If the density does not change and no dead volumes or bypasses occur, the mean residence time is equal to the hydrodynamic residence time, which is calculated from the reactor volume V_R and the particle volume flow rate $\dot{V}_p$:

$$\tau = \frac{V_R}{\dot{V}_p} \tag{4}$$

For the comparison of experiments with different bed masses or process conditions, the dimensionless type of the residence time (θ) is used, which is defined as the ratio of the residence time and the mean residence time:

$$\theta = \frac{t}{\bar{t}} \tag{5}$$

Consequently, the dimensionless exit age distribution $E(\theta)$ is defined as follows:

$$E(\theta) = \bar{t}E(t) \tag{6}$$

Experimental determination of RTD is usually conducted with tracer substances. The tracer is injected with the continuous flow at the reactor inlet and its concentration $c(t)$ or a proportional signal $S(t)$, e.g. the pH value, electric conductivity, or fluorescence, is measured at the outlet:

$$E(t) = \frac{\dot{m}(t)}{m_0} = \frac{\dot{V}c(t)}{\int_0^\infty \dot{V}c(t)\mathrm{d}t} = \frac{c(t)}{\int_0^\infty c(t)\mathrm{d}t} = \frac{S(t)}{\int_0^\infty S(t)\mathrm{d}t} \tag{7}$$

In this study, magnetizable tracer particles were used. These tracer particles can be separated from periodically collected samples by a magnetic rod, allowing a fast measurement of the tracer concentration [7]. The tracer injection can be performed as impulse, step, or periodically or stochastically. In this contribution, the impulse method was used, where the tracer is injected in a very small time interval Δt. In the ideal case, this is a Dirac impulse defined as follows:

$$\int_{-\infty}^{+\infty} \delta(t)\mathrm{d}t = 1 \tag{8}$$

In practice, the time interval Δt should be smaller than 1 % of the mean residence time $\bar{t}$ [8]. Additional requirements for the tracer are the same chemical and physical properties (e.g., density) as the feed material. In addition, the tracer has to be inert, must not adsorb in the process chamber, and it has to be detectable in small amounts and completely miscible with the feed material [9]. All these requirements have been validated for the magnetizable tracer particles before, and it has been proven that the tracer particles and bed material have the same fluidization behavior without any segregation or clustering effects [7].

Residence times in fluidized beds have been experimentally determined for several decades [10–15]. Nevertheless, detailed investigations on continuously operated spouted beds are still rare in the literature.

1) List of symbols at the end of the paper.

For a comparison of the apparatus configurations and the process conditions, several mathematical models for the description of RTD have been developed as, e.g., the tank-in-series model or the dispersion model. The tank-in-series model, which is also called cascade model, was developed in 1935 by MacMullin and Weber [16] and is based on the principle that the RTD of non-ideal reactors can be approximated by a number of ideal reactors. For the description of the distribution with this simple model, only the number of equally sized reactors and the mean residence time are required. In the theory of the axial dispersion model, it is assumed that, in a real plug-flow reactor, the flow of an ideal plug-flow reactor is superimposed by axial dispersion [17]. The dispersion is due to two different phenomena: (1) molecular diffusion compensating for concentration differences and (2) deviations from ideal plug-flow behavior caused by vortices and turbulent velocity variations. Both phenomena are linearly dependent on the concentration gradient and, thereby, the dispersion can be described analogously to the diffusion in Fick's first law [18]:

$$\dot{n}_{\mathrm{disp}} = -AD_{\mathrm{ax}}\frac{\mathrm{d}c}{\mathrm{d}x} \tag{9}$$

with the axial dispersion coefficient D_{ax}, the dispersion flow rate $\dot{n}_{\mathrm{disp}}$, and the concentration c. By means of the material balance after the impulse feeding of tracer material, the following expression is obtained, which is also known as the 1D Fokker-Planck equation [19]:

$$\frac{\partial c_{\mathrm{T}}}{\partial t} = D_{\mathrm{ax}}\frac{\partial^2 c_{\mathrm{T}}}{\partial x^2} - u_{\mathrm{p}}\frac{\partial c_{\mathrm{T}}}{\partial x} \tag{10}$$

with the tracer concentration c_{T} and the particle flow velocity u_{p}. The ratio between the convective and the dispersive transport is expressed by the dimensionless Bodenstein number (Bo), which is equal to the product of the particle velocity and the apparatus length (L_{bed}) divided by the dispersion coefficient (D_{ax}):

$$Bo = \frac{u_{\mathrm{p}}L_{\mathrm{bed}}}{D_{\mathrm{ax}}} \tag{11}$$

By using the Bodenstein number, the dimensionless time θ, and a dimensionless length $X = x/L_{\mathrm{bed}}$, a dimensionless dispersion model is obtained:

$$\frac{\partial C_{\mathrm{T}}}{\partial \theta} = \frac{1}{Bo}\frac{\partial^2 C_{\mathrm{T}}}{\partial X^2} - \frac{\partial C_{\mathrm{T}}}{\partial X} \tag{12}$$

In case of $Bo \to \infty$, the particle flow corresponds to an ideal plug-flow reactor without axial mixing and a dispersion coefficient around zero. In the RTD, a high slim peak occurs. For ideal mixing and a dispersion coefficient tending to infinity, the distribution is broader and flatter. For an open-open system, there is an analytical way to solve the dimensionless dispersion-convection equation. In case of a closed-closed system, which is valid for common fluidized beds as there is no dispersion of particles over the reactor boundaries, there is no analytical solution available. Instead, the equation has to be solved numerically, which has been done by, e.g., Bachmann et al. [20], who proposed a correlation for the dependence of the Bodenstein number by using data from their own experiments and from experiments in the literature. Alternatively, the Bodenstein number can be calculated implicitly with the variance related to the dimensionless residence time, which is defined as:

$$\sigma_\theta^2 = \frac{\sigma^2}{\tau^2} \tag{13}$$

For a closed-closed system, the Bodenstein number has a discontinuity at $X = 0$ and $X = 1$, as no backflow is allowed. Under this assumption, the Bodenstein number can be calculated with Eq. (14) [8].

$$\sigma_\theta^2 = \frac{2}{Bo} - \frac{2}{Bo^2}\left(1 - e^{-Bo}\right) \tag{14}$$

2 Material and Methods

2.1 Pilot-Scale Spouted Bed

The investigated pilot-scale spouted-bed system ProCell *25* of the company Glatt GmbH (Germany) has a prismatic geometry with two parallel gas inlet slits. It contains four stages, the gas volume flow rates and gas temperatures of which can be adjusted individually. In every chamber, a two-fluid nozzle is installed in bottom spray configuration (Fig. 1). For the dry RTD measurements in this contribution, no liquid was injected. Nevertheless, to prevent particles falling into the nozzle tip, nozzle air was applied (0.1 mbar). Particles are inserted at the top of the process chamber on the right-hand side of the apparatus via a rotary valve that is connected with the chamber via a tube. The particles are transported along the bed by the fluid-

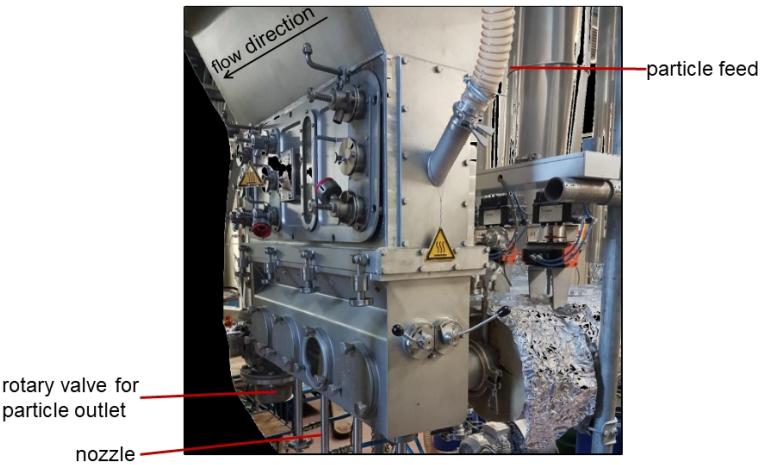

Figure 1. Continuous spouted-bed ProCell 25 (Glatt, Germany) at the Institute of Solids Process Engineering and Particle Technology, TUHH, Hamburg.

ization gas and leave the chamber on the left-hand side of the chamber, slightly above the gas inlet area, through another rotary valve. Besides the original configuration of the apparatus, experiments were performed with separation plates containing mouse holes of varying sizes between the chambers.

In a preliminary study, it was found that the plates need to cover the whole area from the gas inlet slits to the cap, as otherwise the particles flow above the plate. For handling reasons, the plates were inserted in the form of three pieces (Fig. 2): The lowest part had the prismatic form, the second rectangular plate ranged from the process to the expansion chamber, and the third and biggest plate (3) was positioned at the top of the expansion chamber in the broadest part. Experiments without any openings in the plates were performed with colored particles, but particle exchange between the chambers occurred. Thus, the small spaces between the plates and the chamber walls caused by manufacturing tolerances needed to be sealed with plasticine. After sealing, no particle transport was observed when the transfer geometries were closed. Two different transfer geometries were tested in this study: a mouse hole of 1 cm and one of 2 cm in diameter. The holes were inserted in the middle of the lowest plate, with the centers positioned at a height of 4 cm above the bar, as shown in Fig. 2.

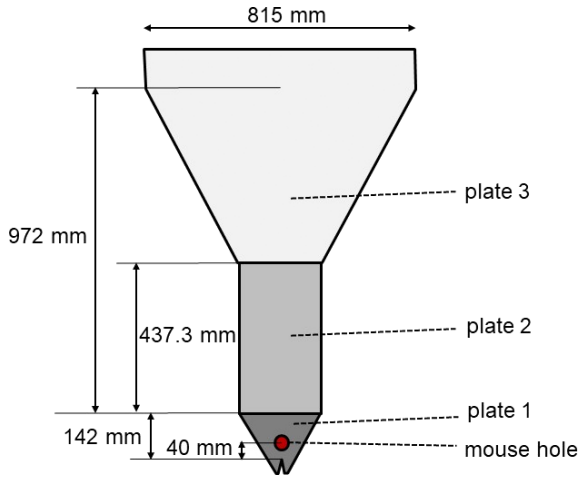

Figure 2. Transfer plates between the different chambers. Each assembly consists of three separate, connected plates.

2.2 Material

The bed material consisted of microcrystalline cellulose particles, Cellets® 500 (Harke Pharma, Germany) with a particle range between 500 and 710 µm and a mean diameter of $d_{50,3} = 589\,\mu m$. With a mean sphericity of 0.96, the particles were almost ideally spherical. Further particle properties, which were determined in the laboratory beforehand, are summarized in Tab. 1. For the production of tracer particles, Cellets® 500 cores were coated with the paint Magneto Grundfarbe (Alpina, Germany), as described in [7].

Table 1. Overview of the properties of the Cellets® 500 particles used for the experiments.

Particle property	Value
Sauter diameter [µm]	631
Apparent particle density [kg m^{-3}]	1481
Bulk density [kg m^{-3}]	764.8
Minimum fluidization velocity [m s^{-1}]	0.14

2.3 RTD Experiments

All presented experiments were performed with a bed mass of 10 kg Cellets® 500 particles in the process chamber and an additional 3 kg in the volume of the outlet rotary valve. A gas volume flow rate of 125 m^{3}h^{-1} was adjusted in every chamber. The particle flow rates at the inlet and the outlet were adjusted to 1 kg min^{-1}. Thus, hydrodynamic residence times of 13 min were expected due to the 10 kg of bed mass in the process chamber and an additional 3 kg in the rotary valve. Each experiment was started when steady-state conditions were reached for several minutes, meaning that a constant flow of 1 kg min^{-1} was inserted into and extracted from the process chamber. At a certain point in time, defined as $t = 0$, the inflow at this very minute consisted of 500 g tracer and 500 g uncoated particles. Tracer injection was performed as fast as possible in order to obtain a short impulse. The outflow of each following minute was collected and used as one sample point for RTD determination. The tracer particles were separated by a magnetic rod (MTN 25/200 N, Sollau s.r.o., Czech Republic) and the weight in each sample was measured.

As the RTD measured in continuous operation do not allow any statement on the history of the particles in the apparatus and the occurrence of backmixing, additional discontinuous experiments were performed for selected configurations. The rotary valves were closed and no in- or outflow was applied. The outlet rotary valve and the four chambers were filled with the partial amount of bed material (3 kg in the rotary valve and 2.5 kg in each chamber), whereby the bed mass of the third chamber contained 500 g tracer particles, as outlined in Fig. 3. This chamber was chosen as it does not have any interactions with the outlet rotary valve. The fluidization of the particles was started (again 125 m^{3}h^{-1} in each chamber). The process was stopped after 2 min, and the tracer distribution as well as the bed mass distribution were measured to determine the mixing behavior in the system.

2.4 Analysis of the Continuous Experiments

After separating the tracer particles from the samples, the exit age distribution is calculated for each time point t_i according to:

$$E(t_i) = \frac{\dot{m}_{T,i}}{m_{T,total}} \tag{15}$$

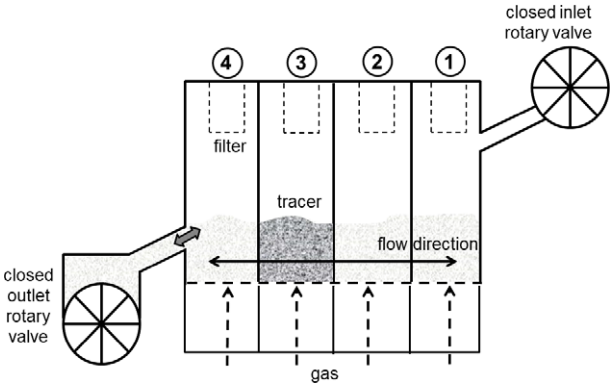

Figure 3. Experimental setup for the qualitative analysis of the axial mixing behavior in the ProCell 25 apparatus. All chambers and the outlet rotary valve were filled with bed material, with the third chamber containing tracer particles. The process was started up and stopped after 10 min of spouting; $\dot{V} = 125\ \mathrm{m^3 h^{-1}}$, $\dot{m}_\mathrm{p} = 1\ \mathrm{kg\ min^{-1}}$.

where $\dot{m}_{\mathrm{T,i}}$ is the amount of tracer in sample i and $m_{\mathrm{T,total}}$ is the total mass of injected tracer. As the regarded process belongs to the group of non-ideal reactors, the residence time is distributed and some particles need a long time to pass the process chamber. Thus, not all tracer particles leave the process within the experimental operation time, meaning that the requirement of Eq. (2) cannot be reached as not all injected tracer particles are collected within the regarded time interval:

$$\int_0^{\mathrm{t,\,end}} E(t)\mathrm{d}t < 1 \tag{16}$$

In order to solve this problem, extrapolation schemes can be applied. In this contribution, the extrapolation is performed with the two-parameter Weibull distribution, which is defined as follows:

$$E_{\mathrm{Weibull}}(t) = \lambda k(\lambda t)^{\mathrm{k}-1} e^{-(\lambda \mathrm{t})^{\mathrm{k}}} \quad \text{for } \tfrac{1}{\lambda} > 0; k > 0 \tag{17}$$

λ is the scale parameter and k is the form parameter, with $\lambda > 0$ and $k = 0$. For $k = 1$, the Weibull distribution resolves the exponential function. For fitting the two parameters to the experimental data, a Weibull mesh is constructed by a double logarithmic application:

$$\ln(-\ln(1 - F(t))) = k\ln(\lambda) + k\ln(t) \tag{18}$$

with $F(t) = \int_0^t E(t)\mathrm{d}t$ being the fraction of particles with a residence time $< t$ in the apparatus.

2.5 Analysis of the Discontinuous Experiments

The horizontal mixing in the discontinuously operated spouted bed can also be described by Fick's second law [21]:

$$\frac{\partial c}{\partial t} = D_{\mathrm{ax}} \frac{\partial c^2}{\partial x^2}, \tag{19}$$

where again c is the concentration and D_{ax} is the dispersion coefficient. For applicability of the model to the measurement data, the boundary condition closed-closed has to be satisfied, meaning that no particle transport through the in- or outlet is possible:

$$t = 0, \quad 0 \le x \le L_1, \quad c = 1 \tag{20}$$

$$t = 0, \quad L_1 \le x \le L_{\mathrm{bed}}, \quad c = 0 \tag{21}$$

$$x = 0, \quad x = L_{\mathrm{bed}}, \quad \frac{\partial c}{\partial x} = 0 \tag{22}$$

with L being the length and L_{bed} the total length of the spouted bed in horizontal direction. For these initial and boundary conditions, the following analytical dependence of the concentration on the dispersion coefficient results as:

$$c(x,t) = \frac{1}{2} + \frac{2}{\pi}\sum_{\mathrm{n}=1}^{\infty} \frac{1}{n} \sin\left(\frac{n\pi}{2}\right) \cos\left(\frac{n\pi x}{L}\right) e^{-\frac{\mathrm{n}^2\pi^2}{\mathrm{L}^2}\mathrm{D_{ax}t}} \tag{23}$$

By fitting Eq. (23) to the experimental data with the sum of least squares method, the dispersion coefficient can be determined and used for the quantification of different process conditions, as shown in the work of Bachmann et al. [20]. A small dispersion coefficient corresponds to a small dispersive and dominant convective flow.

3 Results and Discussion

3.1 RTD Measurements

In a first step, the residence time behavior of the original configuration without any installed plates was measured. The resulting RTD is shown in Fig. 4 in dimensionless form for a clear comparison with the cascade model. After the experiment, about 80 % of the tracer material was found in the samples, giving the need for the Weibull extrapolation scheme described in Sect. 2.4. The mean residence time $\bar{t}$ was calculated from the data as 13.75 min, which is close to the expected hydrodynamic residence time of 13 min, indicating that no bypasses or dead zones occurred.

Deviations from an ideal shape can be seen as small ups and downs are detectable especially at subsequent time points. Nevertheless, a similarity to the density distribution from a continuous stirred-tank reactor is obvious, which is validated by the corresponding dimensionless plot also shown in Fig. 4. The obtained curve has similarities with both the cascade model with only one reactor and that with two reactors, which can be explained by the undefined flow pattern in the outlet rotary valve, resulting in a delayed outflow. The flow behavior in the rotary valve is in-between those of the plug-flow and the continuous stirred-tank reactor (CSTR), as especially near the walls good mixing was observed whereas in the center a tunnel flow was detected. Thus, the rotary valve can, to some extent, be stated as an additional stirred-tank reactor, which causes the measured RTD curve to lie in-between that of a CSTR and that of a cascade consisting of two tanks.

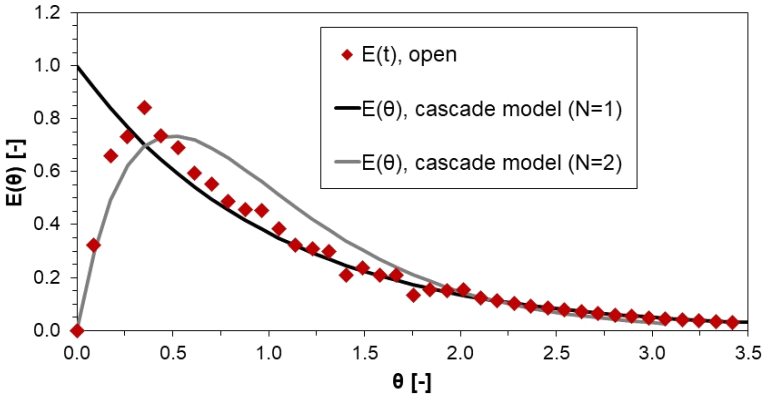

Figure 4. Dimensionless RTD of the original chamber configuration in comparison with the cascade model with one or two CSTR; $\dot{V} = 125\ m^3h^{-1}$, $\dot{m}_p = 1\ kg\ min^{-1}$.

From Fig. 4, two main characteristics of the original chamber configuration can be identified: (1) Tracer particles were already detected after 1 min of operation (= low minimum residence time) and (2) the RTD is very broad. Both aspects are disadvantageous, especially when referring to granulation or coating applications. When particles move directly to the chamber outlet, they do not stay in the spray zone for a sufficient time to be coated with liquid droplets. On the other hand, the broad RTD results in a broad spectrum of exposure duration in the chamber, which comes along with different coating layers and thus inhomogeneous product qualities.

In the next step, experiments with mouse holes were performed. The resulting RTD for both a hole of 1 cm and a hole of 2 cm in diameter and the corresponding extrapolated values are shown in Fig. 5. The data are shown in dimensional form, for reasons of clarity of the absolute minimum residence times.

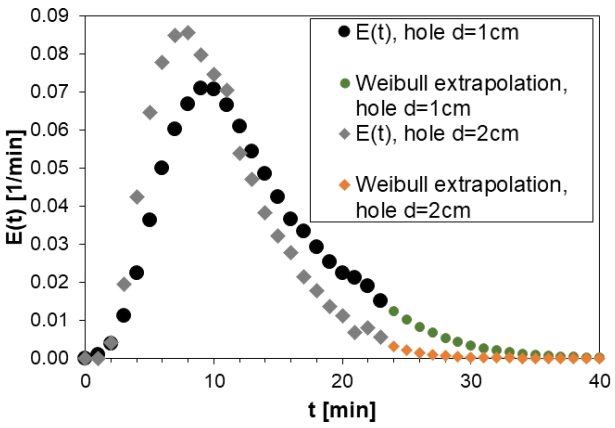

Figure 5. RTD measured with magnetizable tracer particles in the configurations with the mouse holes (1 and 2 cm in diameter) as transfer geometry of the continuously operated ProCell 25 and the corresponding Weibull extrapolation of the experimental data; $\dot{V} = 125\ m^3h^{-1}$, $\dot{m}_p = 1\ kg\ min^{-1}$.

Obviously, the above-mentioned drawbacks with the original configuration could be reduced: The minimum residence time is increased and the distribution itself is slimmer. Both changes are advantageous for obtaining a more homogeneous product quality in any kind of spouted-bed application. Thus, the residence time behavior was positively changed by the installed plates. Comparing the two distributions in Fig. 5, a slimmer curve can be observed for the bigger hole. During process operation with the smaller hole, the time interval of the outflow needed to be extended during the experiment as otherwise the flow rate could not be maintained anymore. This indicates that the opening diameter of 1 cm is too small for the desired flow rate. This assumption is confirmed by the bed mass distribution after the experiment, which shows a strong material accumulation in the first chamber and almost no material in the fourth chamber (Fig. 6). Thus, the smaller hole size is not suitable for the desired process conditions as the cross-section is not big enough to enable the particle transport of 1 kg min^{-1}.

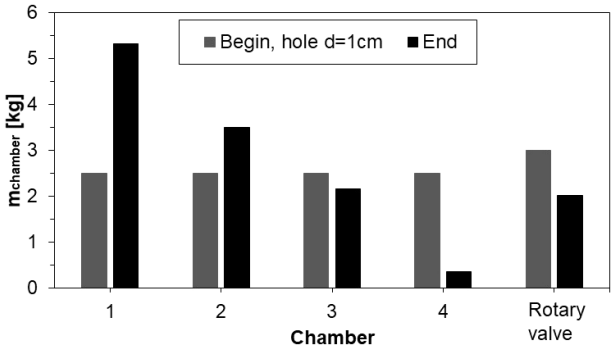

Figure 6. Bed mass distribution at the beginning and the end of continuous operation of the ProCell 25 with the hole configuration: hole diameter = 1 cm; $\dot{V} = 125\ m^3h^{-1}$, $\dot{m}_p = 1\ kg\ min^{-1}$.

For quantitative comparison of the chamber configurations, the Bodenstein number is calculated for each experiment (Tab. 2). With the plates, the Bodenstein numbers are markedly increased compared to the original chamber, indicating a lower axial dispersion and thus backmixing. Nevertheless, the Bodenstein number does not provide any information about the backmixing itself. Thus, discontinuous experiments, as described in Sect. 2.3, were performed to further investigate the flow pattern. These experiments were performed with the bigger hole, as with the small hole the flow rate could not be maintained.

Table 2. Bodenstein numbers calculated from the residence time measurements in the continuously operated pilot-scale spouted-bed ProCell 25.

Configuration	Bodenstein number [–]
Original, no separation plates	0.36
Mouse hole, $d = 1$ cm	4.77
Mouse hole, $d = 2$ cm	4.4

3.2 Discontinuous Operation

The tracer concentrations in the chambers and the rotary valve after the experiment with the bigger hole ($d = 2$ cm) are plotted in Fig. 7. It can be seen that the backmixing was not avoided with the mouse hole. Instead, even slightly higher concentrations of tracer were detected in the backwards direction compared to the chambers in forward direction. Nevertheless, this difference can also be related to the transient behavior of the spouted bed. In total, it is assumed that the mouse hole comes along with a random flow pattern without any preferred flow direction in case that no convective particle flow is applied.

In order to validate the assumption of an almost equal movement of particles into the forward and backward direction, the bed mass distribution was measured after the experiment (Fig. 8). Obviously, the bed mass is almost constantly distributed, which again indicates that the backmixing is not suppressed by the hole itself. As the minimum residence time and the Bodenstein number could be increased with the plates, it can be concluded that a chamber separation reduces the dispersive flow into the outflow region during continuous operation. In contrast, when no convective flow is applied, the chamber separation with the mouse hole does not result in a particle movement to the outflow. Instead, the particle flow into the forward direction is just as likely as that into the backward direction. In order to enhance the forward movement, a transfer geometry with a partly inclined plate is proposed to avoid particles being able to move backwards again.

After the qualitative description of the influence of the plates with the mouse hole, a quantitative value for the axial dispersion was calculated by a changed experimental setup: As the flow behavior in the outlet rotary valve is not predictable, the valve was closed. In addition, the process was started up and the tracer was injected into the running spouted bed into the fourth chamber. Again, the experiment was conducted for 2 min and the tracer distribution was measured afterwards. Analogously to the explanations in Sect. 2.5, initial conditions are defined according to the setup, with L_1 being the length of the fourth chamber and L_{bed} being the length of the whole spouted bed. The dimensionless concentration is determined by correlating the tracer mass concentration to the concentration at the beginning of the experiment:

$$C = \frac{c_T}{c_{T,0}} \tag{24}$$

As mentioned before, the dispersion coefficient is obtained by means of the least squares method, meaning that the residual sum of squares of the experimental data and the objective function is minimized. The obtained experimental data of the dimensionless tracer concentration and the fitted curve with the corresponding dispersion coefficient are shown in Fig. 9.

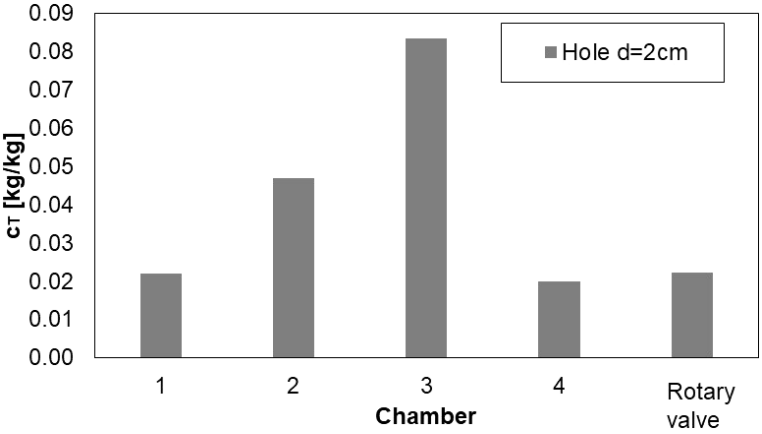

Figure 7. Tracer concentrations in the different parts of the ProCell 25 apparatus with the transfer plate containing a hole ($d = 2$ cm), after discontinuous operation for 2 min; $\dot{V} = 125\ m^3h^{-1}$, $\dot{m}_p = 1\ kg\ min^{-1}$.

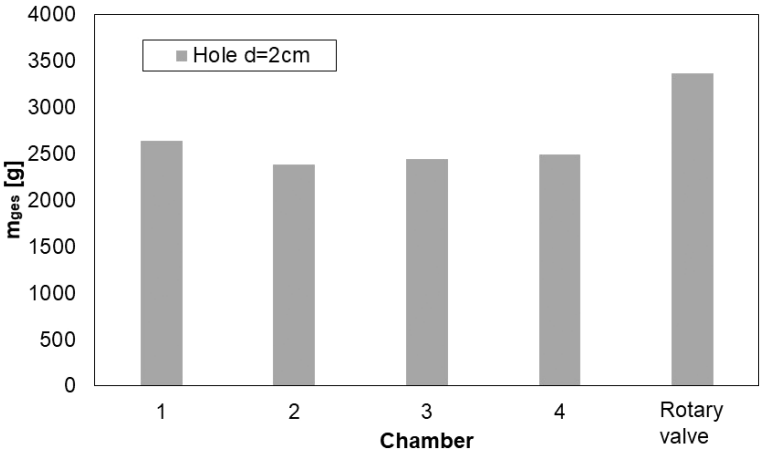

Figure 8. Bed mass distribution in the different parts of the ProCell 25 apparatus with the transfer plate containing a hole ($d = 2$ cm), after discontinuous operation for 2 min; $\dot{V} = 125\ m^3h^{-1}$, $\dot{m}_p = 1\ kg\ min^{-1}$.

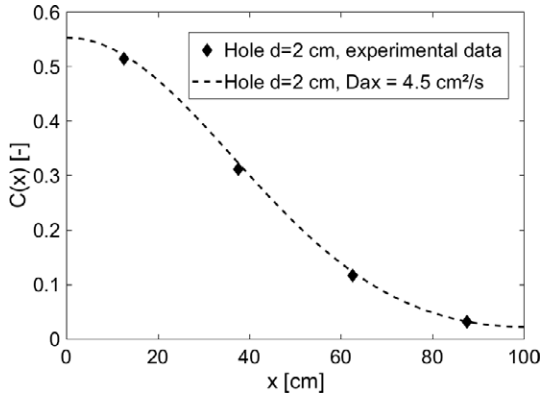

Figure 9. Fitting of the experimental data to the equation of dispersion for the configuration: mouse hole, $d = 2$ cm; minimum sum of the least squares method: 2.19×10^{-4}.

The obtained value for the dispersion coefficient is in the range of those reported in the literature for fluidized beds, e.g. by Shi and Fan [22] or Bachmann and Tsotsas [15]. Thus, and due to the very low value of the minimum sum of the least squares method (2.19×10^{-4}), it can be concluded that the applied dispersion model is also applicable to spouted beds and that the values can be determined by performing discontinuous experiments.

Besides the chosen standard condition of 125 m^3h^{-1} ($u-u_{mf}$ = 0.59 $m\,s^{-1}$), two other gas volume flow rates, namely 90 m^3h^{-1} ($u-u_{mf}$ = 0.42 $m\,s^{-1}$) and 160 m^3h^{-1} ($u-u_{mf}$ = 0.75 $m\,s^{-1}$) were tested regarding the influence of the gas velocity on the backmixing. From Fig. 10, it can be seen that the dispersive flow is increased with increasing gas volume flow rate, which meets the expectations as the increased spouting velocity results in a higher transfer probability due to the increased particle mobility. The dependence is almost linear. This trend was also found by Kato et al. [23] and Shi and Fan [22] for fluidized beds.

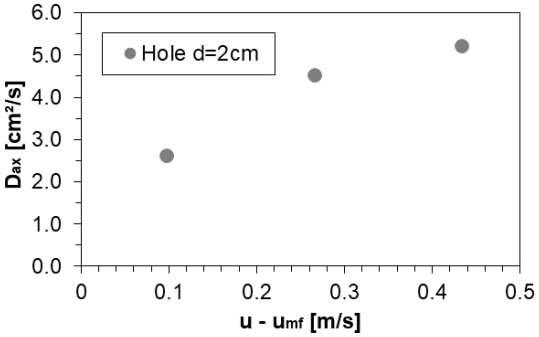

Figure 10. Experimentally determined dispersion coefficients for the discontinuously operated ProCell 25 apparatus with the transfer plate containing a mouse hole (d = 2 cm) in dependence on the gas velocity.

4 Conclusions

RTD measurements were performed in a continuously operated ProCell 25 with magnetizable tracer particles. The residence time behavior can be positively influenced by the installation of plates reaching from the bottom to the top of the apparatus with a mouse hole of 2 cm in diameter in the prismatic part. A smaller mouse hole of 1 cm in diameter cannot be used, as the desired mass flow rate can then not be maintained. The mouse hole with a diameter of 2 cm resulted in an increased minimum residence time and a narrower RTD with, at the same time, a reduced axial dispersion indicated by the Bodenstein number, in comparison to the configuration without plates between the chambers. By discontinuous experiments, it was shown that the backmixing is not reduced by the holes if no convective flow is applied. Thus, it is summarized that a plate with an inclined plane should be used if particle backmixing should be further reduced, as particles are then inhibited from moving backwards against the inclination.

The authors have declared no conflict of interest.

Symbols used

$C(x)$	[–]	dimensionless concentration
$c(t)$	[kg kg^{-1}]	concentration
c_T	[kg kg^{-1}]	tracer concentration
d	[m]	diameter
D_{ax}	[m^2s^{-1}]	axial dispersion coefficient
$E(t)$	[s^{-1}]	exit age distribution (density distribution)
$F(t)$	[–]	sum distribution of the residence time
k	[–]	form parameter of the Weibull extrapolation
L	[m]	length of the spouted bed
L_{bed}	[m]	total length of the spouted-bed apparatus
m_0	[kg]	initial mass
$\dot{m}(t)$	[kg s^{-1}]	mass flow rate
$\dot{n}_{disp}$	[mol s^{-1}]	dispersion flow rate
$S(t)$	[S m^{-1}], e.g.	proportional signal
t	[s]	time
$\bar{t}$	[s]	mean residence time
Δt	[s]	time interval
u_{mf}	[m s^{-1}]	minimum fluidization velocity
u_p	[m s^{-1}]	particle velocity
$\dot{V}$	[m^3s^{-1}]	volume flow rate
V_R	[m^3]	reactor volume
x	[m]	x-coordinate
X	[–]	dimensionless length

Greek symbols

θ	[–]	dimensionless residence time
λ	[–]	scale parameter of the Weibull extrapolation
μ_1	[s]	first moment of the exit age distribution
σ^2	[Pa]	empirical variance, second moment
τ	[s]	hydrodynamic residence time (space time)

References

[1] P. Basu, S. A. Fraser, *Circulating Fluidized Bed Boilers*, Springer, New York **1991**.
[2] K. B. Mathur, P. E. Gishler, *AIChE J.* **1955**, *1 (2)*, 157–164. DOI: https://doi.org/10.1002/aic.690010205
[3] *Spouted and Spout-Fluid Beds: Fundamentals and Applications: Scaleup, Slot-Rectangular, and Multiple Spouting* (Eds: N. Epstein, J. R. Grace), Cambridge University Press, Cambridge and New York **2011**.
[4] *Company Brochure*, Glatt Ingenieurtechnik GmbH, Wiesbaden **2006**.
[5] O. Levenspiel, *Chemical Reaction Engineering*, 3rd ed., Wiley, Hoboken **1999**.
[6] P. V. Danckwerts, *Chem. Eng. Sci.* **1953**, *2 (1)*, 1–13. DOI: https://doi.org/10.1016/0009-2509(53)80001-1

[7] S. Pietsch, P. Kieckhefen, M. Müller, M. Schönherr, F. Kleine Jäger, S. Heinrich, *Powder Technol.* **2018**, *338*, 1–6. DOI: https://doi.org/10.1016/j.powtec.2018.06.040
[8] M. Baerns, *Technische Chemie*, Wiley-VCH, Weinheim **2006**.
[9] E. Salamí, Einfluss verschiedener Parameter auf die Verweilzeitverteilung in einem Strömungsrohr, *Ph.D. Thesis*, ETH Zurich, **1968**.
[10] M. Jacob, Experimentelle Untersuchung sowie Beiträge zur Modellierung von Prozessen in Wirbelschichtrinnen am Beispiel der Sprühgranulation, *Ph.D. Thesis*, Universität Magdeburg, Magdeburg **2010**.
[11] S. Satija, I. L. Zucker, *Drying Technol.* **1986**, *4 (1)*, 19–43. DOI: https://doi.org/10.1080/07373938608916309
[12] R. L. Hull, A. E. von Rosenberg, *J. Ind. Eng. Chem.* **1960**, *52 (12)*, 989–992.
[13] L. Nilsson, R. Wimmerstedt, *Chem. Eng. Sci.* **1988**, *43 (5)*, 1153–1160.
[14] V. Idakiev, L. Mörl, *J. Chem. Technol. Metall.* **2013**, *48 (5)*, 451–456.
[15] P. Bachmann, E. Tsotsas, *Procedia Eng.* **2015**, *102*, 790–798.
[16] R. B. MacMullin, M. Weber, *Trans. Am. Inst. Chem. Eng.* **1935**, *31 (2)*, 409–458.
[17] S. Li, F. Xin, L. Li, *Reaction Engineering*, Elsevier Science, Amsterdam **2017**.
[18] P. Atkins, J. de Paula, *Physical Chemistry for the Life Sciences*, Oxford University Press, USA **2011**.
[19] H. Risken, *The Fokker-Planck Equation: Methods of Solution and Applications*, 2nd ed., Springer Series in Synergetics, Vol. 18, Springer, Berlin, Heidelberg **1996**.
[20] P. Bachmann, A. Bück, E. Tsotsas, *Powder Technol.* **2016**, *301*, 1067–1076. DOI: https://doi.org/10.1016/j.powtec.2016.07.045
[21] A. Fick, *J. Membr. Sci.* **1995**, *100 (1)*, 33–38. DOI: https://doi.org/10.1016/0376-7388(94)00230-V
[22] Y.-F. Shi, L. T. Fan, *Powder Technol.* **1985**, *41 (1)*, 23–28. DOI: https://doi.org/10.1016/0032-5910(85)85070-1
[23] K. Kato, Y. Sato, D. Taneda, T. Sugawa, *J. Chem. Eng. Jpn.* **1985**, *18 (3)*, 254–261.

